



Energy and exergy analysis of biogas fired regenerative gas turbine cycle with CO₂ recirculation for oxy-fuel combustion power generation



Mohammadreza Mohammadpour^a, Ehsan Houshfar^{a,*}, Mehdi Ashjaee^a, Amirreza Mohammadpour^b

^a School of Mechanical Engineering, College of Engineering, University of Tehran, P.O. Box 11155-4563, Tehran, Iran

^b Faculty of Mechanical Engineering, Tarbiat Modares University, Tehran, Iran

ARTICLE INFO

Article history:

Received 6 May 2020

Received in revised form

9 October 2020

Accepted 20 December 2020

Available online 30 December 2020

Keywords:

Biogas

Oxy-combustion

Gas turbine

CO₂ capture and storage

Chemical equilibrium

Exergy analysis

ABSTRACT

In this paper, thermodynamic performance of oxy-biogas regenerative gas turbine cycle with CO₂ recirculation is evaluated. The CO₂ stream is split into the primary and dilution zones. In the primary zone, chemical-equilibrium-model is applied for exergy analysis. Influences of relevant parameters—CO₂-to-O₂ molar ratio (CtO) in the primary zone and primary diluent ratio (PDR)—on the temperature of combustion chamber (CC) and turbine, net produced power, thermal efficiency, specific fuel consumption (SFC) and CO₂ capturing mass flow rate are studied. Decreasing CtO and raising PDR result in high net produced power. Thermal efficiency has a maximum value in the range of CtO (1.5<CtO<4.0) and PDR (0.2<PDR<0.6) and by enhancing CtO, exergy destruction diminishes in both zones. With increasing the CtO in the range of 1.5–2.98, thermal efficiency is increased by 9.92% while variation of CtO in the range of 2.98–4 results in reduction of thermal efficiency by 1.3%. In the range of PDR, the minimum value of SFC is 388 g/kWh and in the range of CtO, the lowest achievable SFC is 387.4 g/kWh. Additionally, dilution zone exergy destruction and CC exergy efficiency increases with PDR and CtO. The two-zone model provided an appropriate control on the turbine inlet temperature.

© 2020 Elsevier Ltd. All rights reserved.

1. Introduction

Although greenhouse gases play the main role in preventing heat from leaving the earth's atmosphere and avoiding the earth to get cooler, an increasing amount of greenhouse gases will result in global warming [1]. Carbon dioxide (CO₂) has a major role in greenhouse effects. This gas is mainly produced by burning fossil fuels and biomass and human activities [1,2]. As a result, the increment of CO₂ concentration in the atmosphere has become one of the major challenges nowadays. In this regard, wide efforts have been made to decrease CO₂ emissions into the atmosphere. To that end, capturing the CO₂ emitted from the power systems [3–6], recycling CO₂ [7], and oxy-fuel combustion are among the recently developed techniques [6]. In an oxy-fuel system, CO₂ may be easily separated from combustion products. Since fuel is burned with oxygen (O₂) instead of air as an oxidizer in the combustion

chamber, the combustion products are CO₂ and steam (H₂O) mainly. In a subsequent process steam can be condensed and separated from CO₂; thus CO₂ can be captured and stored [8]. Also, the application of gas turbines as power generator in various industries such as power plants is an important way in the production of clean energy compared to other power generation systems such as coal burning systems. Another way to reduce greenhouse effects is to utilize renewable energy such as bioenergy sources, e.g. biofuels [9,10]. Compared to fossil fuels, energy from waste resources and biogas declines the chance of possible emission of greenhouse gases to the atmosphere [11]. Various researches have been carried out on application of biofuels in gas turbine power plant and performance enhancement of gas turbine power cycles, among which are reviewed as follows:

Khan et al. conducted extensive researches about performance enhancement of gas turbine power cycles from energy and exergy points of view [12–14]. Bruno et al. [15] carried out analysis on biogas-based integrated energy systems including micro gas turbine (MGT) and absorption cooling system. The study applied

* Corresponding author.

E-mail address: houshfar@ut.ac.ir (E. Houshfar).

Nomenclature			
c_p	Specific heat capacity at constant pressure (kJ/kg·K)	x_i	Number of moles for <i>i</i> th species (mol)
c_v	Specific heat capacity at constant volume (kJ/kg·K)	y_i	Mole fraction of <i>i</i> th gas species
\bar{c}_p	Molar specific heat capacity at constant pressure (kJ/kmol·K)	<i>Greek Symbols</i>	
\bar{c}_v	Molar specific heat capacity at constant volume (kJ/kmol·K)	ε	Molar ratio of primary diluent and oxidizer gas mixture to fuel
\dot{E}_x	Total exergy (kW)	η	First law efficiency
ex	Specific exergy (kJ/kg)	η_{II}	Exergy efficiency
ΔG_j^0	Standard state Gibbs free energy change for species <i>j</i> (kJ/kmol)	φ_p	Primary zone equivalence ratio
h	Enthalpy (kJ/kg)	λ_{CC}	Combustor pressure loss parameter
\bar{h}_i	Molar enthalpy for species <i>i</i> (kJ/kmol)	<i>Abbreviations</i>	
\bar{h}_{mix}	Molar enthalpy of gas mixture (kJ/kmol)	CC	Combustion chamber
$K_{p,j}$	Equilibrium constant for species <i>j</i>	CtO	CO ₂ to O ₂ molar ratio
k	Heat capacity ratio	FOC	Fuel-oxygen and carbon dioxide mixture ratio
M	Molar mass	MGT	Micro gas turbine
\dot{m}	Mass flowrate (kg/s)	ORC	Organic Rankine Cycle
\dot{m}_{fuel}	Fuel mass flowrate (kg/s)	PDR	Primary diluent ratio
\dot{m}_{ox}	Oxygen mass flowrate (kg/s)	SDR	Secondary diluent ratio
N_{tot}	Total number of moles in combustion products (mol)	SFC	Specific fuel consumption (g/kWh)
Q_{in}	Input heat to the combustor (kJ)	TIT	Turbine inlet temperature (K)
p	Pressure (Pa)	LHV	Lower heating value
q	Real heat transfer in regenerator (kJ)	<i>Subscripts</i>	
q_{max}	Maximum heat transfer in regenerator (kJ)	comp	Compressor
r_p	Pressure ratio	ch	Chemical
R_u	Universal gas constant (J/kmol·K)	ph	Physical
s_i	Entropy for species <i>i</i> (kJ/kg·K)	dil	Dilution
T	Temperature (K)	reg	Regeneration
\dot{W}_{net}	Net produced power (kW)	pri	Primary zone
\dot{w}	Specific power of the turbine (kJ/kg)	s	Isentropic
X	Molar ratio of CO ₂ to O ₂	th	Thermal
		tur	Turbine

absorption chillers in to biogas-driven MGT to enhance the system performance. Amiri and Najafabadi [16] conducted a research on energy, exergy and environmental analysis of gas turbine power cycle by using a mixture of biogas and natural gas as fuel. The study examined the effect of biogas to natural gas mass flow rate (BNR) ratio on system performance, cycle efficiency, and NO_x pollutants. Results of the study showed that by increasing BNR, energy and exergy efficiencies of the system enhances and higher value of BNR leads to decrease NO_x emissions. In a later study carried out by Leonzio [17] on an innovative trigeneration power plant which consists of a mechanical compression heat pump, an absorption heat pump, a steam plant, and a heat recovery plant to produce cooling, heating, and electricity. The system was fed with biogas as a renewable energy source. Sevinchan et al. [18] investigated energy and exergy analyses of a novel biogas-based multigenerational system to produce electricity, heating, and cooling. The system has different sub systems such as an open-type Brayton cycle, an organic Rankine cycle (ORC), and a two-stage biomass digester. Results of the study showed that the overall energy efficiency of energy system was 72.5%. Hosseini et al. [19] analysed an integrated biogas-fired micro-power generation system from thermodynamic point of view. The effects of design parameters such as air compressor pressure ratio on energy and exergy efficiency were investigated. It was reported that the overall energy and exergy efficiencies of the system decrease with the compressor pressure ratio. Comparative analysis of the feasible condition for combined heat and power (CHP) and combined cycle based on a 5 MW gas

turbine with biogas fuel was investigated by Kang et al. [20] from an economic perspective. Also, different heat demand patterns and selling prices were considered in economic analysis of the proposed system. Main purpose of the study was economic analysis of the system with detailed temperature dependent thermodynamic performance evaluation. Also, the study considered monthly and hourly variations in fuel consumption, electric power generation, and heat supply capacity in the economic evaluation of the proposed power plant. The study reported that by increasing ambient temperature, power and heat supplied by the system reduces.

Zareh et al. [21] performed thermodynamic and exergoeconomic analysis of a heat and power cogeneration system that operates on blended biogas and natural gas. The first law efficiency and total specific cost of the system were considered as the objective functions to evaluate the effect of burning biogas and natural gas on economics and efficiencies of the selected power plant. Results of the study showed that, the total cost rate of the cogeneration power plant rises as the inlet temperature of gas turbine increases. Gholizadeh et al. [22] developed a new power generation system comprised of a modified organic Rankine cycle and a gas turbine, in which the system was fed by biogas. In the study, thermodynamic and thermo-economic assessments were carried out to evaluate the cost and performance of the system. Combustion chamber had the maximum exergy destruction rate. It was further shown that thermal efficiency can be maximized by applying optimum value of compression ratio. Gholizadeh et al. [23] conducted an investigation on design and simulation of a

biogas-based combined cooling and power system from energetic and exergetic points of view. The effects of input parameters such as compression ratio and fuel composition on the system performance were evaluated. The results of exergy analysis showed that combustion chamber has the highest exergy destruction among all the components of the proposed energy system. Sung et al. [24] carried out thermodynamic analysis on combined MGT and bottoming organic Rankine cycle which operates on biogas from food waste treatment and sewage sludge. The study considered the key parameters including the annual utilization ratio and the net present value (NPV) to analyse the proposed power plant from an economic perspective. Also, analysis of the effect of biogas methane ratio on economic parameters of the proposed system such as NPV was carried out. Results of the study showed that NPV and utilization ratio increases by enhancing biogas methane ratio.

Various studies on oxy fuel power plants have been conducted. Oxy-fuel combustion is a technology which affects energy system's performance. Self et al. [25] investigated the impacts of oxy fuel combustion on the performance of steam power plant using waste heat from oxy-fuel and air-fuel combustion system. Results of the study showed that by utilizing oxy fuel combustion technology, system performance improves with respect to air fuel combustion mode. Mathieu and Nihart [26] investigated a novel oxy-fuel cycle consisting supercritical CO₂ Rankine and regenerative CO₂ Brayton cycle. The study aimed at introducing a zero emission CO₂ cycle with high efficiency. Nami et al. [27] presented a combined zero emission energy system involving S-Graz oxy-fuel cycle, geothermal based organic Rankine cycle, proton exchange membrane electrolyzer, and methanol synthesis unit. The proposed system was analysed from energy and exergy perspectives. Saeidi et al. [28] investigated an oxy-fuel cycle (MATIANT cycle) integrated with gasification unit from energy and exergy points of view. The aim of the study was to remove CO₂ emission from the combustion products and thereby store and transport it. Also, a parametric study was conducted to analysis of system performance. The study reported that increasing gas turbine's inlet pressure results in higher system performance. Soltanieh et al. [29] carried out economic analysis of a zero emission integrated system to co-produce electricity and methanol. The proposed system includes water electrolysis plant, MATIANT oxy-fuel system, and methanol synthesis unit. The CO₂ captured from the oxy-fuel plant reacts with hydrogen derived from the water electrolysis unit and generates methanol. In the study, both the total cost of product and CO₂ emission to the environment were estimated. Thermodynamic assessment and optimization of a natural-gas-based oxy-combustion system (Allam cycle) was investigated by Scaccabarozzi et al. [30].

Xiang et al. [31] presented an energy system based on oxy-fuel combustion technology called natural gas combined cycle (NGCC). The proposed system operated on natural gas with CO₂ and H₂O as an oxidizer. The effects of different fuel-oxidizer arrangements on net power of the system were investigated. Moreover, the study considered the effect of recycled CO₂ flow rate on the system performance. Mehrpooya and Sharifzadeh [32] studied a combined energy system including LNG cold recovery, oxy-fuel cycle, and high temperature solar cycle by energetic and exergetic approaches. Results of the study revealed that the oxy-fuel-based subsystem performed role of capturing CO₂. Some key parameters like turbine inlet temperature (TIT) and LNG flow rate were considered to analyse the system performance. Ghorbani et al. [33] assessed performance of an integrated energy system composed of absorption refrigerant system, oxy-fuel power plant, and water desalination system. The proposed system was fuelled by natural gas, and the aim of the study was to produce liquid natural gas and desalinate water with CO₂ capturing. The heat and power which were

produced by oxy fuel power plant was used in refrigerant system and desalination unit. A part of natural gas was applied to the oxy combustion cycle to produce power and the remaining fuel is used to provide required cooling demand for the refrigeration cycle of liquefied natural gas (LNG) production. Xiang et al. [34] studied oxy fuel combustion power plant from energy and exergy perspectives. The system operated on natural gas with O₂/H₂O as the oxidizer. The system efficiency at various H₂O phase state (liquid water, steam, liquid-steam mixture) was investigated. The study concluded that the mixture of steam-water state is the best state to control the combustion temperature. Shan et al. [35] studied a hybrid energy system consists of oxy-fuel thermo-photovoltaic device with a Brayton and organic Rankine cycles (ORC). The effects of different working fluids in ORC such as R123 and n-pentane and combustion conditions such as oxygen concentration on power generation of proposed energy system were studied. Maddahi and Hossainpour [36] investigated coal based oxy-fuel energy system integrated with organic Rankine cycle, thermodynamically and economically. The selected power system components studied comprised of steam generator unit, oxygen separation unit, compression unit and ORC. Also, study considered ORC to recover waste heat. Sundkvist et al. [37] conducted a study on natural gas based oxy-fuel gas turbine combined cycles. The study simulated combustion chamber by considering two zone models including primary zone and secondary zone. In the study, working fluid (mainly CO₂ and H₂O) was considered to decrease and stabilize the flame temperature.

In this paper, a novel biogas-based regenerative gas turbine power cycle operated on oxy combustion conditions is studied from energy and exergy analyses point of view. This study contributes to existing researches on thermodynamic modelling of combustion within gas turbine's combustion chamber and makes an important opportunity to advance the understanding of chemical equilibrium models for oxy combustion process in biogas powered gas turbines. In this study, Gas turbine combustion chamber is considered in two different zones, namely, primary and dilution. This is because the two-zone model is more reliable than a single zone one in which there is possibility of analysing the effect of diluent mass flow rate on the power cycle thermodynamic performance. In the primary zone, equilibrium combustion model is used instead of complete combustion because of high temperature (above 2000 K) in which dissociation of combustion products and accordingly heat absorption is notable [38]. As presented by previous researches, the highest exergy destruction occurs in the combustion chamber. Hence, detailed exergy analysis considering chemical and physical parts of exergy destruction in each CC zones has been carried out. Based on the stated approach, effects of relevant parameters involving Primary diluent ratio (PDR) and CO₂ to O₂ molar ratio (X) on the temperature of combustion zones, performance parameters such as cycle net power, thermal efficiency, mass flow rate of stored CO₂ stream, and CC exergy destruction are investigated.

2. Methodology

2.1. Model description

In this section, energy and exergy assessments of the selected system are discussed. For evaluating the thermodynamic performance of the plant, each components of the proposed system is considered as a distinct control volume in order to satisfy mass and energy balances. The governing equations are solved using the Engineering Equation Solver (EES) software. A set of algebraic nonlinear equations are being solved simultaneously by extended Newton's method in EES [39]. The nonlinear equations can be defined as following:

$$f = \begin{bmatrix} f_1(x_1, x_2, \dots, x_n) \\ f_2(x_1, x_2, \dots, x_n) \\ \vdots \\ f_n(x_1, x_2, \dots, x_n) \end{bmatrix} \quad (1)$$

The Jacobi matrix will be a $n \times n$ matrix for a set of n algebraic equations and n unknowns. The components of the Jacobian matrix include the partial derivative of the nonlinear equations with respect to unknowns. The Jacobian matrix can be defined as following:

$$J = \begin{bmatrix} \frac{\partial f_1(x_1, x_2, \dots, x_n)}{\partial x_1} & \dots & \frac{\partial f_1(x_1, x_2, \dots, x_n)}{\partial x_n} \\ \frac{\partial f_2(x_1, x_2, \dots, x_n)}{\partial x_1} & \dots & \frac{\partial f_2(x_1, x_2, \dots, x_n)}{\partial x_n} \\ \vdots & & \vdots \\ \frac{\partial f_n(x_1, x_2, \dots, x_n)}{\partial x_1} & \dots & \frac{\partial f_n(x_1, x_2, \dots, x_n)}{\partial x_n} \end{bmatrix} \quad (2)$$

The unknowns can be obtained as following:

$$\begin{bmatrix} x_1^{i+1} \\ x_2^{i+1} \\ \vdots \\ x_n^{i+1} \end{bmatrix} = \begin{bmatrix} x_1^i \\ x_2^i \\ \vdots \\ x_n^i \end{bmatrix} + J^{-1}f\alpha \quad (3)$$

where J^{-1} denotes the inverse of the Jacobian matrix and α is a factor which its value is between 0 and 1. By considering initial guesses for unknown variables, the iterative process starts and repeats until the residual reaches to specified relative tolerance.

2.2. Power plant configuration

Fig. 1 represents a biogas-based oxy-fuel power plant that is composed of an oxy-fuel combustion chamber (CC), compressor, turbine, regenerator, splitter, and H₂O separator. As shown in Fig. 1, CO₂ stream enters the compressor and after pressure rises due to compression is being used as a dilution agent for the combustion process. To preheat the CO₂ stream prior to combustion, a regenerator is used. CC includes two main zones: primary and dilution. As represented in Fig. 2, biogas and pure oxygen are fed to the primary zone in which the combustion reactions occur. Pure oxygen is assumed to be supplied from oxygen production unit which includes Solar driven solid oxide electrolyzer cell (SOEC) [40,41]. However, modelling and analysis of the CCS and oxygen production units are not considered and the effects of energy consumption of the oxygen production and carbon capture and storage units on the system performance are not considered in this study, and therefore is a valuable topic to be addressed in further researches. A fraction of the compressed CO₂ stream is used to reduce the high temperature, which is caused because of using pure oxygen instead of air as oxidizer in the primary zone. After the primary zone, temperature of the combustion products is still far beyond the allowable temperature of turbine blades, which is why the remaining fraction of compressor outlet CO₂ stream is used to dilute and reduce the temperature of the hot combustion products before entering the turbine. Expansion of combustion products generates power in the

cycle. Exhaust stream of the turbine which is a mixture of CO₂ and H₂O is then used to preheat the outlet stream of the compressor in the regenerator. After regenerator, H₂O is condensed and separated from CO₂ in a rather simple condenser. The additional CO₂ in the stream which is produced in the CC is removed and sent to a CO₂ capture and storage unit and the remaining fraction of the stream is recirculated to the CC through the compressor. The temperature-entropy diagram of the proposed power plant is exhibited in Fig. 3. It should be noted that the mass flow rate is not the same in the six indicated states.

To simulate and analyse the proposed system, the following assumptions are considered:

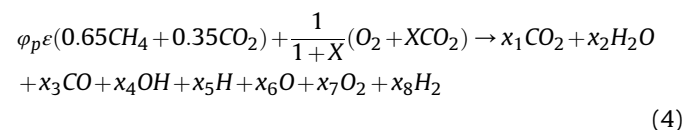
- all components of the oxy-fuel power system are modelled in a steady-state condition.
- pressure drop in the preheater is negligible.
- the biogas fuel is composed of 65% CH₄ and 35% CO₂ (by mole) and the combustion is adiabatic.
- the ideal gas mixture law is applied to model the combustion products.

2.3. Combustion analysis

The model of combustor in gas turbine engine consists of two distinct zones: primary and dilution. In the primary zone, combustion reactions take place and in the dilution zone, gas temperature is lowered to the TIT using diluent. Models used for description of each zone are presented as follows.

2.3.1. Primary zone

In the primary zone, biogas is burnt with mixture of O₂ and CO₂. So, the overall chemical equation of the combustion reaction can be written as follows:



In Equation (4), x_1 to x_8 denote the number of moles for each species. Also, X represents molar ratio of CO₂ to O₂ in the primary diluent and oxidizer gas mixture and, φ_p shows primary zone equivalence ratio which is the ratio of actual fuel-oxygen and carbon dioxide mixture ratio (FOC_s) to the stoichiometric fuel-oxygen and carbon dioxide mixture ratio (FOC) and ε is the molar ratio of primary diluent and oxidizer gas mixture to fuel in the stoichiometric combustion of the fuel which is obtained by:

$$\varphi_p = \frac{FOC}{FOC_s} \quad (5)$$

$$\varepsilon = \frac{1}{1.3(1+X)} \quad (6)$$

From Equation (4), eight unknown mole numbers of products (x_1-x_8) are needed to solve the problem. Three unknowns can be calculated by atom balance of carbon, hydrogen, and oxygen (C, H, O), and the five remaining should be obtained by assuming chemical equilibrium in the product gas mixture. The five chemical equations based on the criteria of equilibrium are assumed to be [42]:

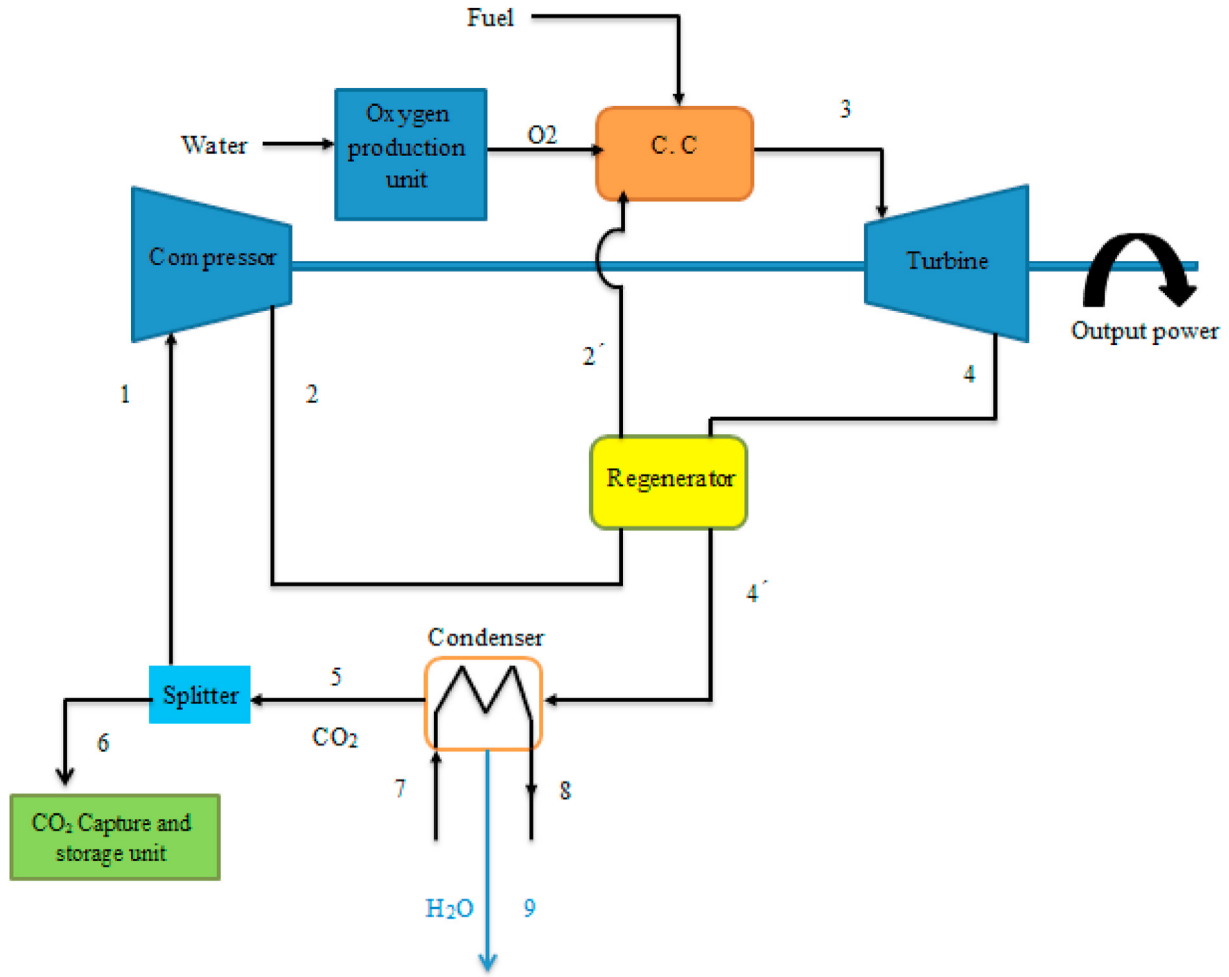


Fig. 1. Oxy-biogas gas turbine power plant with CO₂ recycling.

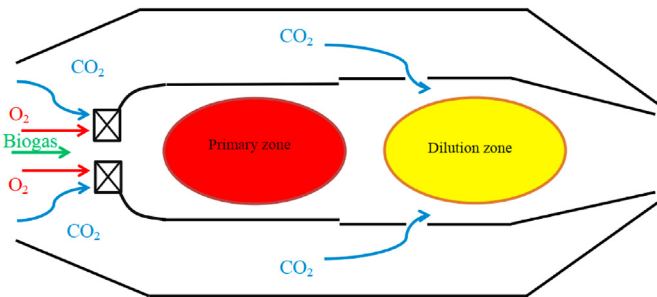


Fig. 2. Schematic model of oxy-fuel combustion chamber.

$$CO + \frac{1}{2}O_2 \rightleftharpoons CO_2, K_{p,4} = \frac{P_{CO_2}}{P_{O_2}^{\frac{1}{2}}P_{CO}} = \frac{y_{CO_2}P^{-\frac{1}{2}}}{y_{O_2}^{\frac{1}{2}}y_{CO}} \quad (10)$$

$$H_2 + \frac{1}{2}O_2 \rightleftharpoons H_2O, K_{p,5} = \frac{P_{H_2O}}{P_{O_2}^{\frac{1}{2}}P_{H_2}} = \frac{y_{H_2O}P^{-\frac{1}{2}}}{y_{O_2}^{\frac{1}{2}}y_{H_2}} \quad (11)$$

where P indicates the total pressure of species and $(K_{p,1}...K_{p,5})$ are defined as the equilibrium constants. Also, y_i represents the mole fraction of i th species that is related to mole number of products:

$$y_i = \frac{x_i}{N_{tot}} \quad (12)$$

From Equation (12), N_{tot} denotes the total number of moles in product gas mixture. To determine the equilibrium constant by means of the standard state Gibbs free energy change ΔG_j^0 , for j th reaction, the following equation is utilized:

$$K_{p,j} = e^{-\frac{\Delta G_j^0}{R_u T}} \quad (13)$$

Based on the chemical reaction in Equation (4), three atom balances for carbon, hydrogen and oxygen can be written as follows [42]:

$$\frac{1}{2}H_2 \rightleftharpoons H, K_{p,1} = \frac{P_H}{P_{H_2}^{\frac{1}{2}}} = \frac{y_H P^{\frac{1}{2}}}{y_{H_2}^{\frac{1}{2}}} \quad (7)$$

$$\frac{1}{2}O_2 \rightleftharpoons O, K_{p,2} = \frac{P_O}{P_{O_2}^{\frac{1}{2}}} = \frac{y_O P^{\frac{1}{2}}}{y_{O_2}^{\frac{1}{2}}} \quad (8)$$

$$\frac{1}{2}H_2 + \frac{1}{2}O_2 \rightleftharpoons OH, K_{p,3} = \frac{P_{OH}}{P_{O_2}^{\frac{1}{2}}P_{H_2}^{\frac{1}{2}}} = \frac{y_{OH}}{y_{O_2}^{\frac{1}{2}}y_{H_2}^{\frac{1}{2}}} \quad (9)$$

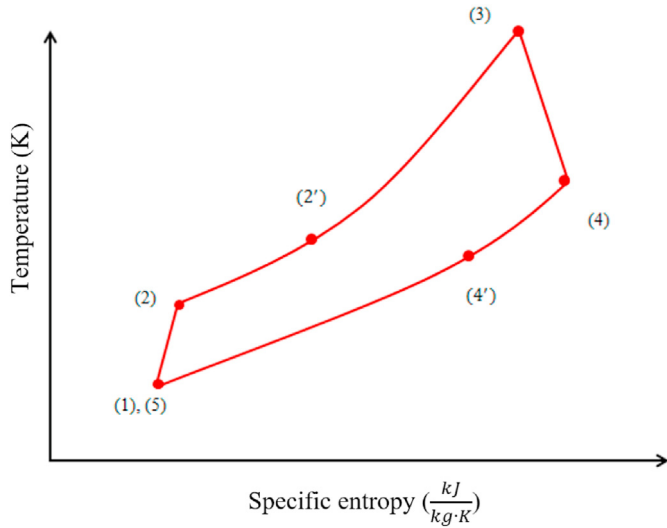


Fig. 3. Temperature-specific entropy diagram of oxy-biogas gas turbine power plant.

$$C: \quad \varphi_p \varepsilon (0.65 + 0.35) + \frac{X}{1+X} = (y_1 + y_3) N_{tot} \quad (14)$$

$$H: \quad 4\varphi_p \varepsilon (0.65) = 2(2y_2 + y_4 + y_5 + 2y_8) N_{tot} \quad (15)$$

$$O: \quad 2\varphi_p \varepsilon (0.35) + \frac{2}{1+X} + \frac{2X}{1+X} = (2y_1 + y_2 + y_3 + y_4 + y_6 + 2y_7) N_{tot} \quad (16)$$

Due to the definition of mole fractions, one more equation is defined as follows:

$$\sum_{i=1}^8 (y_i) = 1 \quad (17)$$

Enthalpy of the mixture based on mole and mass of the mixture can be calculated by Ref. [43]:

$$\bar{h}_{mix} = \sum_{i=1}^8 (y_i \bar{h}_i) \quad [kJ / kmol] \quad (18)$$

$$h_{mix} = \frac{1}{M} \sum_{i=1}^8 (y_i \bar{h}_i) \quad [kJ / kg] \quad (19)$$

Also, the molar specific heat capacity of the mixture at constant pressure and constant volume is respectively expressed by:

$$\bar{c}_{p,mix} = \sum_{i=1}^8 (y_i \bar{c}_{p,i}) \quad [kJ / kmol \cdot K] \quad (20)$$

$$\bar{c}_{v,mix} = \sum_{i=1}^8 (y_i \bar{c}_{v,i}) \quad [kJ / kmol \cdot K] \quad (21)$$

where M is molar mass of the mixture and defined as:

$$M = \sum_{i=1}^8 (y_i M_i) \quad [kg / kmol] \quad (22)$$

Specific heat, enthalpy and entropy values of each gaseous species are function of temperature and can be calculated using the following expressions. The coefficients of the relations can be obtained from thermodynamic tables reported by McBride et al. [44]:

$$\frac{c_{p,i}(T)}{R_u} = a_{1,i} T^{-2} + a_{2,i} T^{-1} + a_{3,i} + a_{4,i} T + a_{5,i} T^2 + a_{6,i} T^3 + a_{7,i} T^4 \quad (23)$$

$$\begin{aligned} \frac{h_i(T)}{R_u T} = & -a_{1,i} T^{-2} + a_{2,i} \frac{\ln T}{T} + a_{3,i} + a_{4,i} \frac{T}{2} + a_{5,i} \frac{T^2}{3} + a_{6,i} \frac{T^3}{4} \\ & + a_{7,i} \frac{T^4}{5} + \frac{b_{1,i}}{T} \end{aligned} \quad (24)$$

$$\begin{aligned} \frac{s_i(T)}{R_u} = & -a_{1,i} \frac{T^{-2}}{2} - a_{2,i} T^{-1} + a_{3,i} \ln T + a_{4,i} T + a_{5,i} \frac{T^2}{2} \\ & + a_{6,i} \frac{T^3}{3} + a_{7,i} \frac{T^4}{4} + b_{2,i} \end{aligned} \quad (25)$$

The amount of input heat in the CC during the combustion process can be expressed by Equation (26) where LHV is the lower heating value of the biogas fuel, which is 20.19 MJ/kg, η_{cc} is the combustor efficiency and \dot{m}_{fuel} is the mass flow rate of the inlet fuel to the combustor:

$$\dot{Q}_{in} = \dot{m}_{fuel} LHV \eta_{cc} \quad (26)$$

For considering pressure loss in the CC, outlet pressure of the combustor is related to its inlet pressure using pressure loss parameter, λ_{CC} , using Eq. (27):

$$P_3 = (1 - \lambda_{CC}) P_2 \quad (27)$$

2.3.2. Dilution zone

After the combustion of fuel and oxidizer in the primary zone, the remaining CO_2 stream from the compressor enters the dilution zone and mixes with hot combustion products leaving the flame zone. Dilution process is essential for providing sufficient volume flow for turbine and making sure TIT is suitable for blade material [45]. Mass flow rates of CO_2 stream in primary and dilution zone are related through the following equation to the total outlet mass flow rate of compressor:

$$PDR + SDR = 1 \quad (28)$$

Hence, the ratios of diluent mass flow rate in the primary and dilution zone to the total compressor mass flow rate are defined as primary diluent ratio (PDR) and secondary diluent ratio (SDR) according to the following equations:

$$PDR = \frac{\dot{m}_{CO_2,pri}}{\dot{m}_{comp}} \quad (29)$$

$$SDR = \frac{\dot{m}_{CO_2,dil}}{\dot{m}_{comp}} \quad (30)$$

After dilution, TIT is calculated by:

$$TIT = T_3 = \frac{(\dot{m}_{CO_2,pri} + \dot{m}_{ox} + \dot{m}_{fuel})c_{p,mix,pri}T_{pri} + \dot{m}_{CO_2,dil}c_{p,2'}T_{2'}}{(\dot{m}_{CO_2,pri} + \dot{m}_{ox} + \dot{m}_{fuel})c_{p,mix,pri} + \dot{m}_{CO_2,dil}c_{p,2'}} \quad (31)$$

where \dot{m}_{ox} is the mass flow rate of oxygen in the primary zone, $c_{p,mix,pri}$ is specific heat capacity of the mixture in the primary zone, $c_{p,2'}$ specific heat capacity of the diluent stream of regenerator and $T_{2'}$ is the temperature of the heated diluent stream.

2.4. Regeneration process

The CO₂ stream at compressor's outlet is preheated before injects into the CC to increase the system overall efficiency. So, due to preheating process, the amount of actual heat exchange rate in the regenerator can be defined as below:

$$q = C_{p,c}(T_{2'} - T_2) = C_{p,mix,h}(T_4 - T_4') \quad (32)$$

where $C_{p,c} = \dot{m}_{comp}c_{p,c}$ and $C_{p,mix,h} = (\dot{m}_{ox} + \dot{m}_{fuel} + \dot{m}_{comp})c_{p,h}$ are cold and hot stream heat capacity rates of regenerator, respectively. Also, the maximum possible heat transfer rate in the regenerator is obtained by:

$$q_{max} = C_{p,min}(T_4 - T_2) \quad (33)$$

In which $C_{p,min}$ is a minimum value between $C_{p,c}$ and $C_{p,mix,h}$. In the compression process, CO₂ is pressurized by the compressor from the first state (ambient temperature and pressure) to the second state. To calculate temperature at the second state, the following equation is considered:

$$\frac{T_{2s}}{T_1} = \left(\frac{P_2}{P_1}\right)^{\frac{k-1}{k}} \quad (34)$$

where $\frac{P_2}{P_1}$ is the pressure ratio and is defined as r_p . T_{2s} is temperature of CO₂ after the ideal isentropic compression. k denotes the ratio of molar specific heat capacity at constant pressure to molar specific heat capacity at constant volume for a gas. The actual outlet enthalpy of CO₂ after compression is obtained from:

$$h_2 = h_1 + \frac{h_{2s} - h_1}{\eta_{comp}} \quad (35)$$

The relation between q and q_{max} is expressed using the definition of heat transfer effectiveness, η_{reg} [46],:

$$\eta_{reg} = \frac{q}{q_{max}} \quad (36)$$

With knowing the value of heat transfer effectiveness, the outlet temperature of cold and hot streams, $T_{out,c}$ and $T_{out,h}$, can be calculated from Eqs. (32) and (36).

2.5. Thermodynamic analyses

2.5.1. Energy analysis

The methodology for evaluation of net output power and cycle efficiency is described in this section. By considering output power of turbine and compressor power consumption, the net power

output produced by the proposed system calculated from:

$$\dot{W}_{net} = \left(\dot{m}_{ox} + \dot{m}_{fuel} + \dot{m}_{CO_2,pri} + \dot{m}_{CO_2,dil}\right)\dot{w}_{tur} - \left(\dot{m}_{CO_2,pri} + \dot{m}_{CO_2,dil}\right)\dot{w}_{comp} \quad (37)$$

The thermal efficiency of the power plant is given by:

$$\eta_{th} = \frac{\dot{W}_{net}}{\dot{Q}_{in}} \quad (38)$$

where \dot{Q}_{in} is introduced in Equation (26). Further, specific fuel consumption (SFC) which is a representative of gas turbine plant economic performance can be defined as:

$$SFC = 3600 \frac{\dot{m}_{fuel}1000}{\dot{W}_{net}} \text{ [g / kWh]} \quad (39)$$

2.5.2. Exergy analysis

Exergy represents the maximum possibilities of a system to produce useful work when it equilibrates with the reference environment state (dead state). Exergy balance can be defined as follows:

$$\dot{Ex}^Q + \sum [\dot{m}_{in}ex_{in}] = \dot{Ex}^w + \sum [\dot{m}_{out}ex_{out}] + \dot{Ex}^D \quad (40)$$

$$\dot{Ex}^Q = \left(1 - \frac{T_0}{T}\right)\dot{Q} \quad (41)$$

$$\dot{Ex}^w = \dot{W} \quad (42)$$

where \dot{Ex}^Q and \dot{Ex}^w denote exergy of heat and exergy of work and \dot{Ex}^D stands exergy destruction and the assumed value for T_0 is 298 K. Exergy of material flow (ex) which includes physical and chemical exergy can be expressed as follows:

$$ex = ex_{ph} + ex_{ch} \quad (43)$$

$$ex_{ph} = \sum y_i [(h - h_0) - T_0(s - s_0)]_i \quad (44)$$

$$ex_{ch} = \sum_{i=1}^N [y_i ex_{ch,i}^0] + RT_0 \sum_{i=1}^N [y_i \ln y_i] \quad (45)$$

where $ex_{ch,i}^0$ represents the standard chemical exergy of the i th gas component. Since the highest rate of exergy destruction occurs in the combustion chamber, special attention should be paid to this part. Hence, the main goal of exergy analysis is to determine the exergy destruction of this equipment. Hence, exergy balance in CC can be written as following [47]:

$$\dot{Ex}_{fuel} + \dot{Ex}_{O_2} + \dot{Ex}_{CO_2,pri} + \dot{Ex}_{CO_2,dil} - \dot{Ex}_{exhaust} = \dot{Ex}^D \quad (46)$$

Also, second law (exergy) efficiency can be evaluated as following:

$$\eta_{II} = 1 - \frac{\dot{E}X^D}{\dot{E}X_{in}} \tag{47}$$

where $\dot{E}X_{in}$ denotes input exergy of the system.

3. RESULTS and DISCUSSION

For evaluation of the thermodynamic performance of the modelled cycle in section 2, computer code was written in the environment of Engineering Equation Solver (EES). Data required for the simulations and default value for variables used in the parametric studies is presented in Table 1. Also, thermodynamic properties in each state point of the proposed power plant are provided on Table 2.

3.1. Oxy-biogas power plant analysis

In the study of thermodynamic performance of oxy-biogas gas turbine power plant, CO₂ to O₂ molar ratio, and primary diluent ratio are considered as two input parameters and the influence of their variation on the temperature of the combustor and turbine, net power produced, thermal efficiency, specific fuel consumption, and CO₂ capture and storage unit inlet mass flow rate are investigated in the following sections. All the results illustrated in the following sections are obtained per unit mass flow rate of CO₂ at the compressor inlet.

3.1.1. CO₂ to O₂ molar ratio effect

Within the CC, the oxygen concentration in the flame zone (primary zone) would be effective on the released heat and consequently the temperature of this zone. Therefore, to control the temperature, an appropriate amount of CO₂ gas should be supplied to the primary zone to dilute the inlet oxygen stream. In this study, parametric analysis is adopted to assess the effect of the CO₂ to O₂ molar ratio (X) on different parameters including temperature of different zones in CC, TIT and TOT (turbine outlet temperature), cycle performance and primary zone inlet mass flow rate. Fig. 4 shows the impact of X on the dilution gas, fuel, and oxygen mass flow rate. It can be inferred that by increasing the value of X from 1.5 to 4, the mass flow rates of fuel and oxygen drop to 62.5% and 20.4%, respectively. Also, it is detected that the primary zone diluent mass flow rate remains constant alongside with the constant PDR. Therefore, in the constant value of PDR, enhancing the value of X means a reduction in oxygen mass flow rate, which consequently results in a decline in the fuel mass flow rate at constant equivalence ratio.

According to Fig. 5 it can be inferred that the variation of X has a significant impact on the temperature of CC zones, TOT and TIT. As expected, growing X from 1.5 to 4 amplifies the dilution effect in the primary zone of the combustor, resulting in a remarkable temperature drop. The temperature reduction in the dilution zone remains approximately at the same value as in the primary zone, but at the

Table 1
Value of parameters required for power plant simulations.

T_0 (°C)25	λ_{cc} 0.025	η_{reg} 0.8
T_1 (°C)25	φ_p 1	r_p 20
T_{fuel} (°C)25	$\eta_{comp,s}$ 0.87	X2.6
T_{O_2} (°C)25	$\eta_{tur,s}$ 0.89	PDR0.3
P_1 (kPa)101.325	η_{cc} 0.99	\dot{m}_{comp} (kg /s)1
P_4 (kPa)101.325	LHV_{Biogas} ($\frac{MJ}{kg}$)20.19	

Table 2
Thermodynamic properties in each state point.

Stream	T (K)	P (bar)	s ($\frac{kJ}{kg \cdot K}$)
1	298	1.013	4.854
2	576.3	20.27	4.917
2'	948.9	20.27	5.486
3	1535	19.76	6.469
4	1042	1.013	6.548
4'	735.9	1.013	6.118
5	298	1.013	4.854
6	298	1.013	4.854
7	283	1.013	10.380
8	313	1.013	10.571
9	317	0.096	11.682

turbine outlet, the temperature drop is less than the previous zones. In fact, the reason for this behaviour is mainly because the rise of X in the combustion zone considering high specific heat capacity of CO₂ which results in more absorption of heat from the combustion and hence, temperature drops for the combustion products.

The influence of X parameter on the plant thermal efficiency and net power produced is displayed in Fig. 6. With the increase of the X value from 1.5 to 4, the net power is reduced by 60.3% from 764.5 kW to 303.7 kW. The reduction of net power occurs because of two main reasons. Firstly, due to the reduction in turbine specific power generation and decrease in temperature difference at the inlet and outlet of turbine, and secondly due to the reduction in turbine inlet mass flow rate. The graph also represents that the thermal efficiency boosts with the growth of X and then falls after reaching a maximum value. This maximum value is 46.5% for X = 2.98. Efficiency enhancement in the range of 1.5–2.98 is mainly because of the heat release decrement in the CC and this can be connected to the reduction in fuel mass flow rate and further reduction in net output power. On the other hand, the reason for efficiency decrement after the maximum value is because the decrement in net output power is greater than the reduction in heat released in the combustor.

The SFC and CO₂ capturing mass flow rate are other important parameters which can be influenced by the X value. According to Fig. 7, the SFC curve has a minimum point with a value of 387.4 g/kWh at X = 2.98. The drop in SFC in the range of 1.5–2.98 is mainly due to the predominance of decrement in fuel mass flow rate on the net output power reduction. Moreover, the SFC growth after the minimum point is because the reduction in net produced power is greater than decrement in fuel mass flow rate. Further, it can be inferred that by increasing X from 1.5 to 4, the CO₂ capturing mass flow rate decreases from 0.099 kg/s to 0.055 kg/s. This is mainly due to reduction of the total exhaust gas mass flow rate and consequently, CO₂ mass flow rate drops at the turbine outlet.

3.1.2. Primary diluent ratio effect

The CO₂ diluent which flows into the CC is divided into two parts, where the first part enters the primary zone and the remainder flows into the secondary zone. The temperature of each zone and the concentration of combustion products depend on the amount of inlet diluent flow into each of the primary and secondary zones. Hence, the fraction of the total diluent flow that enters the primary zone is considered as an input parameter, called PDR, and its effect on the system performance is carried out. Fig. 8 illustrates the influence of PDR on the fuel, oxygen, and primary zone diluent mass flow rate. By rising PDR, the mass flow rate of all three streams increases monotonically. Also, PDR increment at a constant X results in increase in oxygen mass flow rate. Moreover, due to the

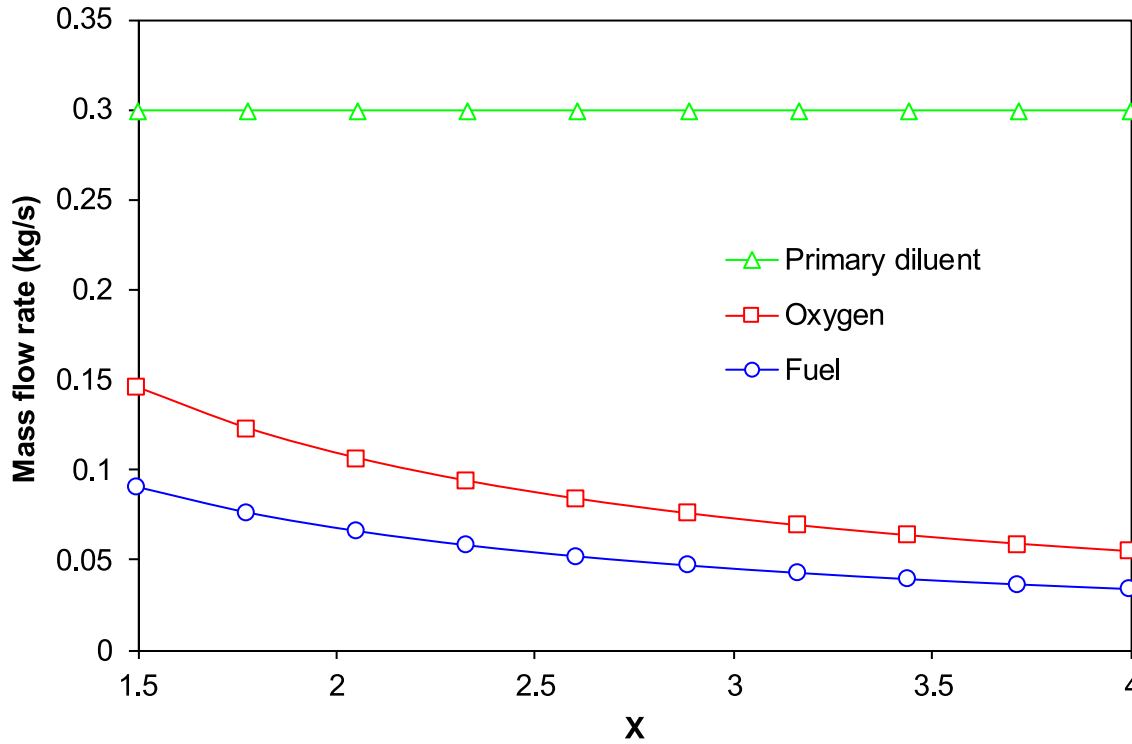


Fig. 4. Fuel, oxygen, and primary diluent mass flow rates versus CO₂ to O₂ molar ratio.

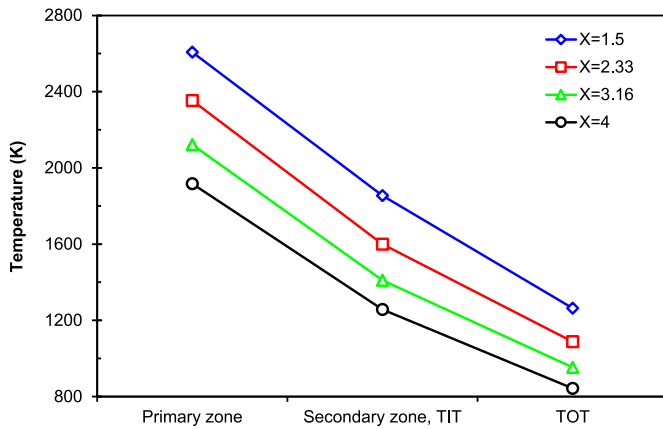


Fig. 5. Temperature variation in the CC and turbine at various CO₂ to O₂ molar ratio.

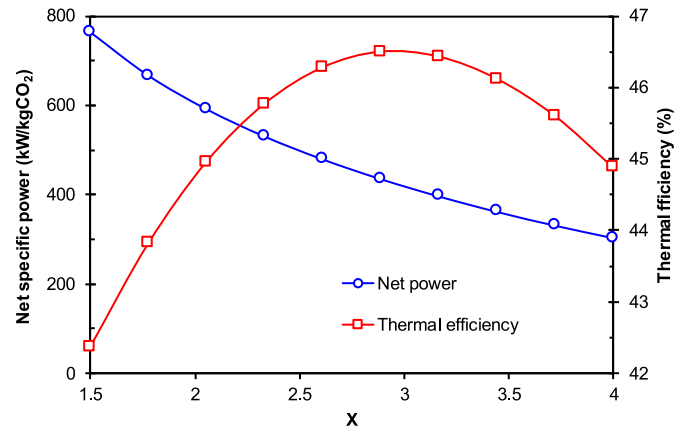


Fig. 6. Net produced power and thermal efficiency variation versus CO₂ to O₂ molar ratio.

constant equivalence ratio, PDR increment leads to a rise in the fuel mass flow rate.

The temperature of different zones and the TIT and TOT are shown in Fig. 9 with respect to PDR. By increasing PDR, the temperature of the primary and secondary zones rises. Furthermore, the temperature changes in the secondary zone is greater than that of the primary zone. The TIT and TOT also increase. At higher PDR, the fuel mass flow rate rises and this leads to heat release augmentation in the combustor. Since increase in PDR leads to fall in the ratio of diluent flow, the cooling effect of diluent stream on the combustion products reduces. Accordingly, this leads to a greater increment in the temperature of the secondary zone compared to the primary zone.

Fig. 10 presents the effect of PDR on the net power produced and thermal efficiency of the plant. By enhancing PDR, the net specific

power rises drastically by 207%. Moreover, thermal efficiency is raised up by increasing PDR from 0.2 to 0.347 and decreases after reaching a maximum point. The maximum value for thermal efficiency is 46.4%. The net output power improvement is due to the increased mass flow rate at the turbine inlet and the higher turbine specific power rising.

The Influence of PDR on SFC and CO₂ capturing mass flow rate is presented in Fig. 11. By changing the PDR value from 0.2 to 0.4, the SFC decreases initially and reaches a minimum point, and then starts to increase. The minimum value for SFC is 388 g/kWh which corresponds to PDR = 0.347. The CO₂ mass flow rate rises uniformly with increasing PDR. This trend may be explained by rising of the output mass flow rate of the combustor and turbine exhaust and accordingly CO₂ mass flow rate growth in the exhaust gases.

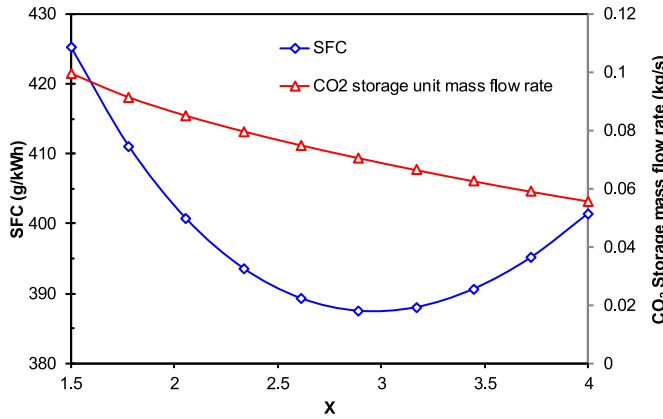


Fig. 7. Specific fuel consumption and CO₂ capturing mass flowrate versus CO₂ to O₂ molar ratio.

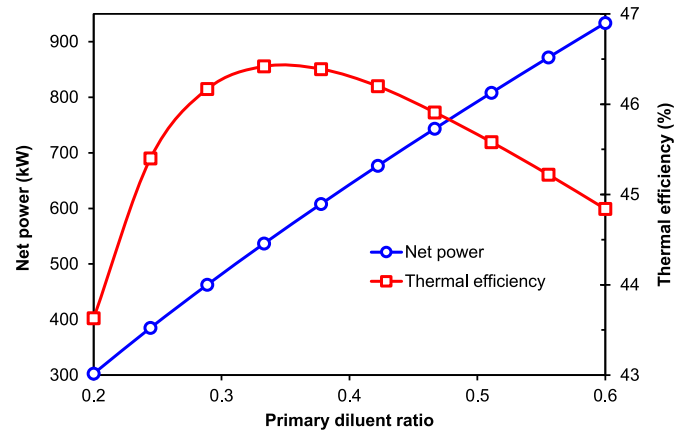


Fig. 10. Net produced power and thermal efficiency variation versus primary diluent ratio.

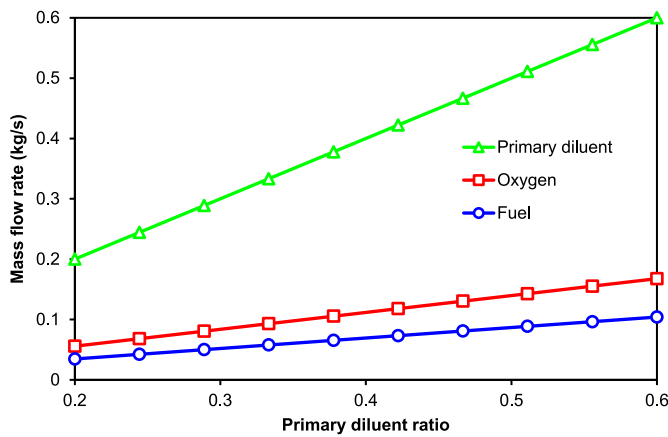


Fig. 8. Fuel, oxygen, and primary diluent mass flowrates versus PDR.

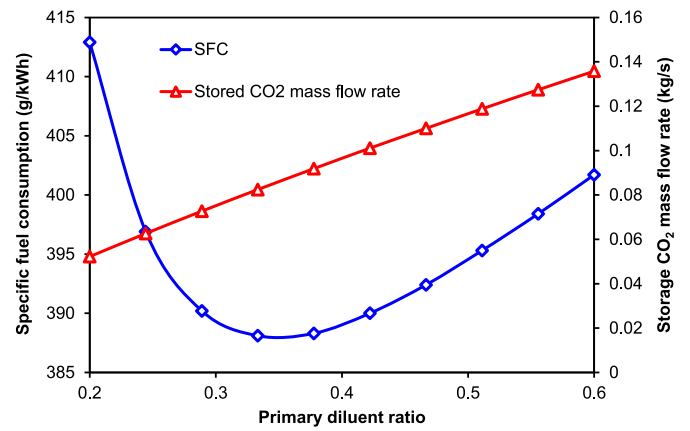


Fig. 11. Specific fuel consumption and CO₂ capture and storage unit inlet mass flowrate versus primary diluent ratio.

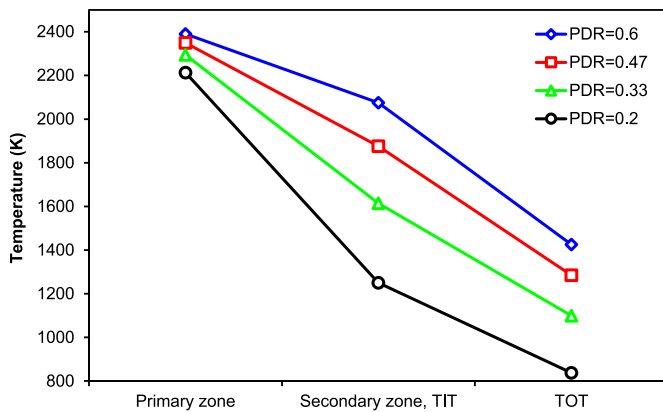


Fig. 9. Temperature variation in the CC and turbine at various primary diluent ratios.

3.2. Validation

Since the model used for the description of CC in the present study consists of two different zones, study of Kayadelen and Ust [48] in which combustion of air-fuel in a non-regenerative steam injected gas turbine cycle was considered in two separate zones (primary and dilution) was selected for validation of results of this study. To compare the results, the case with no steam injection was

considered. Details of different parameters used for validation can be found in Kayadelen and Ust [48]. The value of parameters required for power plant validations are defined in Table 3. As shown in Fig. 12, the net output power and thermal efficiency of the gas turbine cycle obtained from the present model closely match with the reference data, which indicates the validity of the current study.

3.3. Result of exergy analysis

In this section, result of exergy analysis on the combustion process of gas turbine engine is presented.

3.3.1. Result of primary diluent ratio effect

The exergy destruction of CC zones as a function of the PDR is presented in Fig. 13. It is obvious that variation of PDR would affect exergy destruction in each zone of CC. A fall in exergy destruction of dilution zone can be clearly seen for different values of PDR and on the contrary, PDR variation would result in increment of primary zone and combustor total exergy destructions. It is evident that the primary zone exergy destruction takes a leading part of the total exergy destruction at entire PDR range. Physically, increasing PDR leads to enhance CO₂ mass flow rate in primary zone and as a result, the total input exergy rises and subsequently exergy destruction grows. Furthermore, the variation of PDR on combustor exergy efficiency is shown in Fig. 14. In this case, increasing PDR enhances

Table 3
Value of parameters required for power plant validations.

T_{air} ($^{\circ}C$)	15	N_2 to O_2 molar ratio	3.76
T_{fuel} ($^{\circ}C$)	15	φ_p	1.02
P_{air} (kPa)	101.325	$\eta_{comp.s}$	0.87
$P_{Tur, exit}$ (kPa)	101.325	$\eta_{tur.s}$	0.89
λ_{cc}	0.04	η_{cc}	0.99

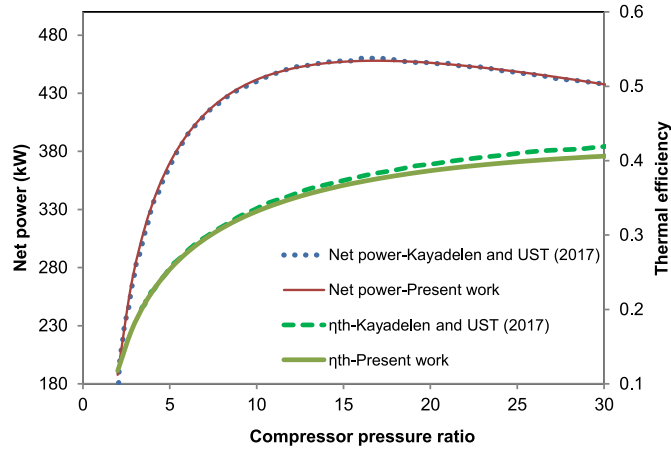


Fig. 12. Comparison between the result of present work and Kayadelen and Ust [48] for net power output and thermal efficiency (N_2 to O_2 molar ratio value: 3.76).

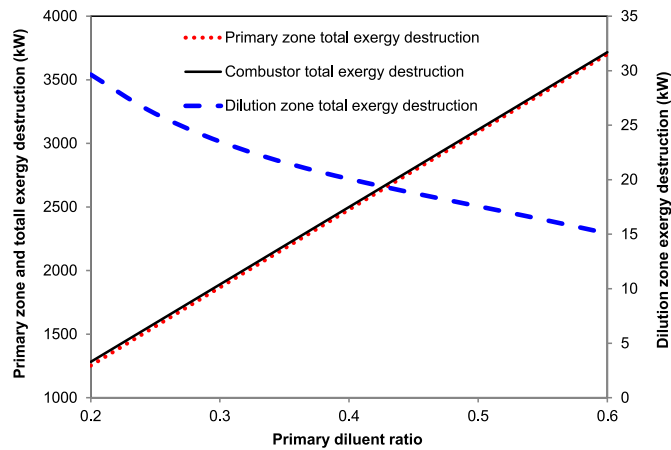


Fig. 13. Effect of primary diluent ratio on exergy destruction in CC zones.

the exergy destruction in the primary zone. In addition, the primary zone exergy destruction is much higher than that of dilution zone due to chemical reactions and extreme temperature differences and hence the total exergy destruction of CC augments and accordingly this leads to reduce exergy efficiency of CC.

3.3.2. Result of CO_2 to O_2 molar ratio effect

It is evident from the Fig. 15 that exergy destruction diminishes by promoting the X value. This trend could be justified by noting that any increase in X value at constant CO_2 mass flow rate leads to decrease in fuel mass flow rate. Therefore, decrement in fuel mass flow rate would reduce the chemical exergy during combustion process. Since exergy destruction mainly occurs because of chemical reactions, accordingly exergy destruction declines by enhancing X. Also, the influence of X on combustor exergy efficiency is presented in Fig. 16. It is evident that enhancing X results

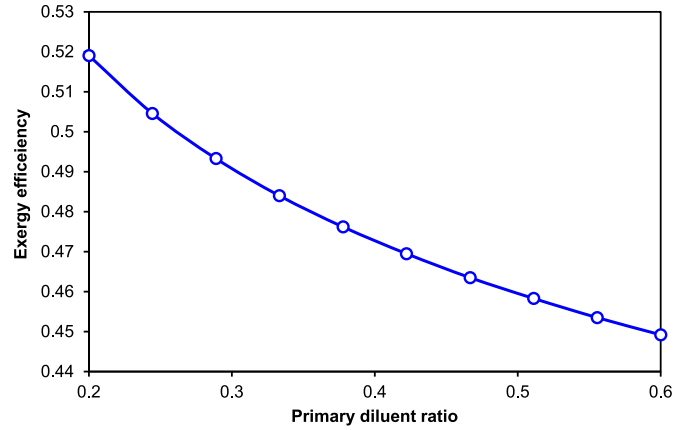


Fig. 14. Effect of primary diluent ratio on combustor exergy efficiency.

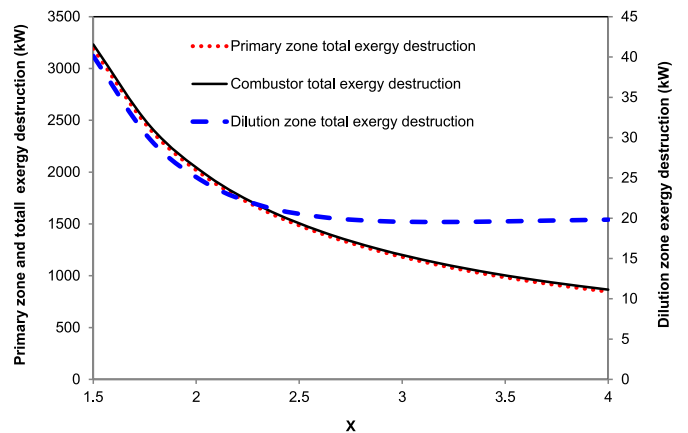


Fig. 15. Effect of CO_2 to O_2 molar ratio on exergy destruction in CC zones.

in exergy efficiency improvement. Here, increasing X diminishes the exergy destruction in the CC zones and due to the predominant contribution of the primary zone irreversibility to the total exergy destruction in CC, the total irreversibility of the CC declines and this leads to enhanced exergy efficiency in the CC.

4. Conclusions

In this study, selected gas turbine power plant with biogas-oxygen combustion and CO_2 recirculation from combustion products to compressor was studied. Cycle performance and CC exergy destruction due to changes in the molar ratio of CO_2 to O_2 in the primary zone and PDR were investigated. A two-zone model was applied to the CC in the gas turbine. In the primary zone, combustion reactions were modelled using chemical equilibrium and in the secondary zone, the combustion products were diluted and their temperature dropped to the TIT. The following conclusions can be drawn from the present study:

- Applying the two-zone model for the CC provides a reliable measure for appropriate control on the turbine inlet temperature over a wide temperature range by examining the effect of changing the diluent flows on the primary and secondary zones.
- Analysis of the influence of CO_2 to O_2 molar ratio shows that reduction in this parameter results in high net output power. Also, at higher PDR, the net output power of the cycle would increase. In the studied range for CO_2 to O_2 molar ratio, the

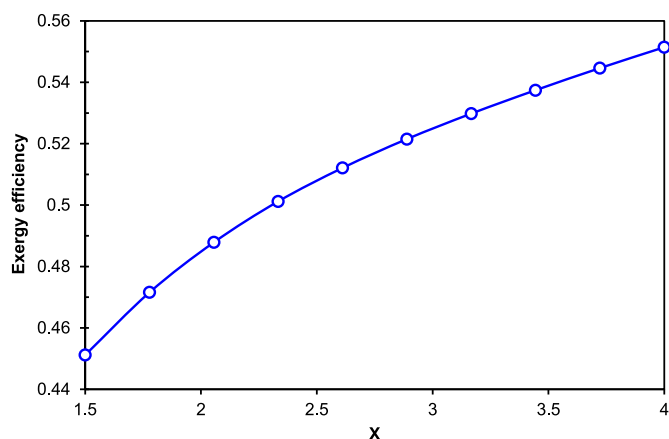


Fig. 16. Effect of CO₂ to O₂ molar ratio on exergy efficiency.

maximum value for thermal efficiency is 46.5%. Similarly, following the variation of the PDR, a maximum value of 46.4% was obtained on the thermal efficiency curve.

- Knowing that SFC is inversely related to thermal efficiency, minimum value of SFC corresponds to the maximum value of the thermal efficiency when the PDR and X are 0.347 and 2.98, respectively.
- The amount of CO₂ mass flow rate that enters the capture and storage unit plays a key role in the plant performance because a higher mass flow rate of CO₂ leads to enhance the compressor consumed power for storage. Increasing the PDR elevates mass flow rate of CO₂ which enters the capture and storage unit but raising the molar ratio of CO₂ to O₂ leads to decline CO₂ mass flow rate which enters to the capturing unit.
- Exergy destruction in the primary zone boosts with the increase of the PDR. Further, by increasing PDR, irreversibility of dilution zone falls. Moreover, with the increase of CO₂ to O₂ molar ratio, exergy destruction diminishes in both CC zones and hence combustor exergy efficiency boosts. Additionally, primary zone exergy destruction plays the main role in total irreversibility of CC due to the chemical reactions and high temperature difference.

CRediT author statement

Mohammadreza Mohammadpour: Conceptualization, Methodology, Formal analysis, Writing – original draft. Ehsan Houshfar: Conceptualization, Writing – review & editing, Supervision, Validation, Visualization. Mehdi Ashjaee: Methodology, Supervision, Project administration, Resources. Amirreza Mohammadpour: Writing – review & editing, Formal analysis, Data reduction.

Declaration of competing interest

The authors declare that they have no known competing financial interests or personal relationships that could have appeared to influence the work reported in this paper.

References

- [1] Huang X, Guo J, Liu Z, Zheng C. Opportunities and challenges of oxy-fuel combustion. In: Zheng C, Liu Z, editors. *Oxy-fuel combustion: fundamentals, theory and practice*. Wuhan, China: Academic Press; 2018. p. 1–12. <https://doi.org/10.1016/B978-0-12-812145-0.00001-3>.
- [2] Dincer I. Renewable energy and sustainable development: a crucial review. *Renew Sustain Energy Rev* 2000;4:157–75. [https://doi.org/10.1016/S1364-0321\(99\)00011-8](https://doi.org/10.1016/S1364-0321(99)00011-8).

- [3] Zhao L, Zhao R, Deng S, Tan Y, Liu Y. Integrating solar Organic Rankine Cycle into a coal-fired power plant with amine-based chemical absorption for CO₂ capture. *Int J Greenh Gas Con* 2014;31:77–86. <https://doi.org/10.1016/j.ijggc.2014.09.025>.
- [4] Zhao R, Deng S, Zhao L, Liu Y, Tan Y. Energy-saving pathway exploration of CCS integrated with solar energy: literature research and comparative analysis. *Energy Convers Manag* 2015;102:66–80. <https://doi.org/10.1016/j.enconman.2015.01.018>.
- [5] Zhao Y, Hong H, Zhang X, Jin H. Integrating mid-temperature solar heat and post-combustion CO₂-capture in a coal-fired power plant. *Solar Energy* 2012;86:3196–204. <https://doi.org/10.1016/j.solener.2012.08.002>.
- [6] Mehrpooya M, Ghorbani B. Introducing a hybrid oxy-fuel power generation and natural gas/carbon dioxide liquefaction process with thermodynamic and economic analysis. *J Clean Prod* 2018;204:1016–33. <https://doi.org/10.1016/j.jclepro.2018.09.007>.
- [7] Habibollahzade A, Houshfar E. Improved performance and environmental indicators of a municipal solid waste fired plant through CO₂ recycling: exergoeconomic assessment and multi-criteria grey wolf optimisation. *Energy Convers Manag* 2020;225:113451. <https://doi.org/10.1016/j.enconman.2020.113451>.
- [8] Jin B, Zhao H, Zheng C. Thermoeconomic cost analysis of CO₂ compression and purification unit in oxy-combustion power plants. *Energy Convers Manag* 2015;106:53–60. <https://doi.org/10.1016/j.enconman.2015.09.014>.
- [9] Sims REH, Rogner H-H, Gregory K. Carbon emission and mitigation cost comparisons between fossil fuel, nuclear and renewable energy resources for electricity generation. *Energy Policy* 2003;31:1315–26. [https://doi.org/10.1016/S0301-4215\(02\)00192-1](https://doi.org/10.1016/S0301-4215(02)00192-1).
- [10] Moharamian A, Soltani S, Rosen MA, Mahmoudi SMS, Morosuk T. A comparative thermoeconomic evaluation of three biomass and biomass-natural gas fired combined cycles using organic Rankine cycles. *J Clean Prod* 2017;161:524–44. <https://doi.org/10.1016/j.jclepro.2017.05.174>.
- [11] Habibollahzade A, Houshfar E, Ahmadi P, Behzadi A, Gholamian E. Exergoeconomic assessment and multi-objective optimization of a solar chimney integrated with waste-to-energy. *Solar Energy* 2018;176:30–41. <https://doi.org/10.1016/j.solener.2018.10.016>.
- [12] Khan M, Alarifi IM, Tlili I. Comparative energy and exergy analysis of proposed gas turbine cycle with simple gas turbine cycle at same operational cost. *ASME international mechanical engineering congress and exposition. American Society of Mechanical Engineers*; 2019. p. 1–9.
- [13] Khan M, Tlili I. Performance enhancement of a combined cycle using heat exchanger bypass control: a thermodynamic investigation. *J Clean Prod* 2018;192:443–52. <https://doi.org/10.1016/j.jclepro.2018.04.272>.
- [14] Khan M. Energy and exergy analyses of regenerative gas turbine air-bottling combined cycle: optimum performance. *Arabian J Sci Eng* 2020;45:5895–905. <https://doi.org/10.1007/s13369-020-04600-9>.
- [15] Bruno JC, Ortega-López V, Coronas A. Integration of absorption cooling systems into micro gas turbine trigeneration systems using biogas: case study of a sewage treatment plant. *Appl Energy* 2009;86:837–47. <https://doi.org/10.1016/j.apenergy.2008.08.007>.
- [16] Rad EA, Kazemiani-Najafabadi P. Introducing a novel optimized Dual Fuel Gas Turbine (DFGT) based on a 4E objective function. *J Clean Prod* 2019;206:944–54. <https://doi.org/10.1016/j.jclepro.2018.09.129>.
- [17] Leonzio G. An innovative trigeneration system using biogas as renewable energy. *Chin J Chem Eng* 2018;26:1179–91. <https://doi.org/10.1016/j.cjche.2017.11.006>.
- [18] Sevinchan E, Dincer I, Lang H. Energy and exergy analyses of a biogas driven multigenerational system. *Energy* 2019;166:715–23. <https://doi.org/10.1016/j.energy.2018.10.085>.
- [19] Hosseini SE, Barzegaravval H, Wahid MA, Ganjehkaviri A, Sies MM. Thermodynamic assessment of integrated biogas-based micro-power generation system. *Energy Convers Manag* 2016;128:104–19. <https://doi.org/10.1016/j.enconman.2016.09.064>.
- [20] Kang JY, Kang DW, Kim TS, Hur KB. Comparative economic analysis of gas turbine-based power generation and combined heat and power systems using biogas fuel. *Energy* 2014;67:309–18. <https://doi.org/10.1016/j.energy.2014.01.009>.
- [21] Darabadi Zareh A, Khoshbakhti Saray R, Mirmasoumi S, Bahlouli K. Extensive thermodynamic and economic analysis of the cogeneration of heat and power system fueled by the blend of natural gas and biogas. *Energy Convers Manag* 2018;164:329–43. <https://doi.org/10.1016/j.enconman.2018.03.003>.
- [22] Gholizadeh T, Vajdi M, Mohammadkhani F. Thermodynamic and thermoeconomic analysis of basic and modified power generation systems fueled by biogas. *Energy Convers Manag* 2019;181:463–75. <https://doi.org/10.1016/j.enconman.2018.12.011>.
- [23] Gholizadeh T, Vajdi M, Rostamzadeh H. Energy and exergy evaluation of a new bi-evaporator electricity/cooling cogeneration system fueled by biogas. *J Clean Prod* 2019;233:1494–509. <https://doi.org/10.1016/j.jclepro.2019.06.086>.
- [24] Sung T, Kim S, Kim KC. Thermoeconomic analysis of a biogas-fueled micro-gas turbine with a bottoming organic Rankine cycle for a sewage sludge and food waste treatment plant in the Republic of Korea. *Appl Therm Eng* 2017;127:963–74. <https://doi.org/10.1016/j.applthermaleng.2017.08.106>.
- [25] Self SJ, Rosen MA, Reddy BV. Effects of oxy-fuel combustion on performance of heat recovery steam generators. *European Journal of Sustainable*

- Development Research 2018;2:22. <https://doi.org/10.20897/ejosdr/69787>.
- [26] Mathieu P, Nihart R. Zero-emission MATIANT cycle. *J Eng Gas Turbines Power* 1999;121:116–20. <https://doi.org/10.1115/1.2816297>.
- [27] Nami H, Ranjbar F, Yari M. Thermodynamic assessment of zero-emission power, hydrogen and methanol production using captured CO₂ from S-Graz oxy-fuel cycle and renewable hydrogen. *Energy Convers Manag* 2018;161:53–65. <https://doi.org/10.1016/j.enconman.2018.01.054>.
- [28] Saeidi S, Mahmoudi SMS, Nami H, Yari M. Energy and exergy analyses of a novel near zero emission plant: combination of MATIANT cycle with gasification unit. *Appl Therm Eng* 2016;108:893–904. <https://doi.org/10.1016/j.applthermaleng.2016.07.095>.
- [29] Soltanieh M, Azar KM, Saber M. Development of a zero emission integrated system for co-production of electricity and methanol through renewable hydrogen and CO₂ capture. *Int J Greenh Gas Con* 2012;7:145–52. <https://doi.org/10.1016/j.ijggc.2012.01.008>.
- [30] Scaccabarozzi R, Gatti M, Martelli E. Thermodynamic analysis and numerical optimization of the NET Power oxy-combustion cycle. *Appl Energy* 2016;178:505–26. <https://doi.org/10.1016/j.apenergy.2016.06.060>.
- [31] Xiang Y, Cai L, Guan Y, Liu W, Han Y, Liang Y. Study on the configuration of bottom cycle in natural gas combined cycle power plants integrated with oxy-fuel combustion. *Appl Energy* 2018;212:465–77. <https://doi.org/10.1016/j.apenergy.2017.12.049>.
- [32] Mehrpooya M, Sharifzadeh MMM. A novel integration of oxy-fuel cycle, high temperature solar cycle and LNG cold recovery – energy and exergy analysis. *Appl Therm Eng* 2017;114:1090–104. <https://doi.org/10.1016/j.applthermaleng.2016.11.163>.
- [33] Ghorbani B, Mehrpooya M, Ghasemzadeh H. Investigation of a hybrid water desalination, oxy-fuel power generation and CO₂ liquefaction process. *Energy* 2018;158:1105–19. <https://doi.org/10.1016/j.energy.2018.06.099>.
- [34] Xiang Y, Cai L, Guan Y, Liu W, Liang Y, Han Y, et al. Influence of H₂O phase state on system efficiency in O₂/H₂O combustion power plant. *Int J Greenh Gas Con* 2018;78:210–7. <https://doi.org/10.1016/j.ijggc.2018.08.006>.
- [35] Shan S, Zhou Z, Cen K. An innovative integrated system concept between oxy-fuel thermo-photovoltaic device and a Brayton-Rankine combined cycle and its preliminary thermodynamic analysis. *Energy Convers Manag* 2019;180:1139–52. <https://doi.org/10.1016/j.enconman.2018.11.040>.
- [36] Maddahi L, Hossainpour S. Thermo-economic evaluation of 300MW coal based oxy-fuel power plant integrated with organic Rankine cycle. *Int J Greenh Gas Con* 2019;88:383–92. <https://doi.org/10.1016/j.ijggc.2019.07.004>.
- [37] Sundkvist SG, Dahlquist A, Janczewski J, Sjödin M, Bysveen M, Ditaranto M, et al. Concept for a combustion system in oxyfuel gas turbine combined cycles. *J Eng Gas Turbines Power* 2014;136. <https://doi.org/10.1115/1.4027296>.
- [38] Lefebvre AH, Ballal DR. *Gas turbine combustion: alternative fuels and emissions*. third ed. Florida, USA: CRC Press; 2010.
- [39] Klein S, Nellis G. *Mastering EES. f-Chart software*; 2012.
- [40] Mohammadi A, Mehrpooya M. Thermodynamic and economic analyses of hydrogen production system using high temperature solid oxide electrolyzer integrated with parabolic trough collector. *J Clean Prod* 2019;212:713–26. <https://doi.org/10.1016/j.jclepro.2018.11.261>.
- [41] Taher MAA. *Model-based evaluation of the integration of solid oxide fuel cells and electrolysis cells for high purity oxygen production*. Imperial College London, PhD thesis; 2017. p. 29–30.
- [42] Kayadelen HK, Ust Y. Prediction of equilibrium products and thermodynamic properties in H₂O injected combustion for C_αH_βO_γN_δ type fuels. *Fuel* 2013;113:389–401. <https://doi.org/10.1016/j.fuel.2013.05.095>.
- [43] Kayadelen HK, Ust Y. Performance and environment as objectives in multi-criterion optimization of steam injected gas turbine cycles. *Appl Therm Eng* 2014;71:184–96. <https://doi.org/10.1016/j.applthermaleng.2014.06.052>.
- [44] McBride BJ, Zehe MJ, Gordon S. *NASA Glenn coefficients for calculating thermodynamic properties of individual species*. 2002.
- [45] Boyce Meherwan P. *Gas turbine engineering handbook*. Houston, TX: Gulf Professional Publishing; 2002.
- [46] Cengel Yag AJ. *Heat and mass transfer: fundamentals and applications*. fifth ed. New York, USA: McGraw-Hill Higher Education; 2014.
- [47] Tsatsaronis G, Morosuk T, Koch D, Sorgenfrei M. Understanding the thermodynamic inefficiencies in combustion processes. *Energy* 2013;62:3–11. <https://doi.org/10.1016/j.energy.2013.04.075>.
- [48] Kayadelen HK, Ust Y. Thermodynamic, environmental and economic performance optimization of simple, regenerative, STIG and RSTIG gas turbine cycles. *Energy* 2017;121:751–71. <https://doi.org/10.1016/j.energy.2017.01.060>.